COMMUNICATION

Programmable Kiri-Kirigami Metamaterials

*Yichao Tang, Gaojian Lin, Shu Yang, Yun Kyu Yi, Randall D. Kamien, and Jie Yin**

There has been tremendous interest in economizing energy use in buildings,[1–3] for example, using smart windows that become opaque to block or reflect sunlight to reduce solar gain and return to a transparent state at a low lighting condition to improve light harvesting.[4–6] However, solutions often require a rather large strain in a switchable optical material to achieve a dramatic transparency change.[5,6] Reconfigurable metamaterials,[7–13] with properties arising from dynamically tunable geometrical structures rather than composition, offer a new material platform to achieve dramatic change of mechanical and optical properties via a relatively modest mechanical stress,[7,14] that lead to unique mechanical behaviors, including buckling induced programmable highly nonlinear mechanical responses,[15] origami-based reprogrammable mechanical metamaterials through lattice defects,[16] and origami-inspired designs of flexibility in deployment and controllable stiffness in transformation.[17–20] While these deformations often occur by compression, highly stretchable and super-conformable metamaterials have been generated by introducing patterned cuts to a rigid, less-stretchable thin sheet.[21–25] This works because cuts allow for "free" rigid rotation[21,22] or out-of-plane buckling of the cut units[23–25] without shearing or stretching the individual units themselves. Cutting and folding together are also referred to as "kirigami". Recently, kirigami structures[26,27] have been exploited as scaffolds to embed rigid electrical and optical components for potential applications, including stretchable and conformable electronics at both large and small scales,[21–24] stretchable batteries,[25] tunable phononic bandgap materials,[16] mechanical self-assembly of 3D mesostructure fabrication,[28] and optical tracking in solar cells.[29] Compared to simple stretching of a flat structured sheet to change transmittance as a responsive building skin,[5,6] kirigami structures can be buckled out of plane with a small strain to reflect or transmit light[28] or heat in response to local changes of solar radiance, lighting, and temperature and represent a potentially new class of adaptive energy-saving building envelopes.[30–32]

To control the tilting angle of individual "louvres" so that they reflect the excess solar radiance from the incoming light, it is important to precisely control the buckling orientation of the kirigami sheet. However, each "louvre" or unit cell in the kirigami structure can buckle up or down—the kirigami structure is mechanically bistable. If not controlled, it would lead to geometric frustration and undesired random disordering.[33,34] Meanwhile, since the direction of the sunlight, the illuminance level, and the amount of solar radiation change during the day and within the building depend on the climate conditions at a specific location, it will be also highly desirable if the kirigami structure can be programmed to achieve multiple configurations, in a controlled fashion. Here, through combined experiments and finite element method (FEM) simulation alongside analytical models, we demonstrate the design of kiri-kirigami (i.e., cuts on cuts)-based metamaterials that can be programmed to tilt into different orientations on demand, as well as potential applications in reflecting or transmitting sunlight as energy efficient building skins.

Figure 1a shows the typical design of kirigami metamaterials with patterned line cuts in a centered rectangular arrangement (see Figure 1a,b). Poly(dimethylsiloxane) (PDMS) is chosen as the sheet material here because it is hyperelastic and thus allows for repetitive elastic loading and unloading without plastic deformation at a large strain.[23,29] Upon stretching the kirigami structure, each cut unit undergoes out-of-plane buckling and tilts into a nearly vertical direction through both bending and twisting accompanied by the opening of a pore. Figure 1c–e shows that the deformed configurations of the kirigami structure (Figure 1a) are highly dependent on the stretching method. When one end of the cut sheet is uniaxially stretched with the other end fixed, all the cut units undergo either a clockwise (represented by "+" in Figure 1c) or counterclockwise rotation (represented by "–" in Figure 1d) depending on which side is fixed (Video S1, Supporting Information). When both ends are stretched simultaneously, the PDMS sheet exhibits a dual tilting orientation with the left half rotating counterclockwise while the right half rotating clockwise, leaving a domain wall in the middle (Figure 1e and Video S1, Supporting Information). Random tilting orientations, if not controlled, could largely degrade the energy saving performance of kirigami-based building envelopes due to uncontrollable light or solar heat reflection or transmission. However, introducing patterned notches to both sides of the kirigami sheet of Figure 1a generates a modified and engineered kirigami structure. To differentiate it from the kirigami structure, we call it a kiri-kirigami structure due to the introduced shallow cuts as demonstrated in Figure 1b. In contrast, the entire kiri-kirigami sheet exhibits homogeneous rotation along the cut units as designed, independent of the stretching conditions

Y. Tang, G. Lin, Prof. J. Yin
Applied Mechanics of Materials Laboratory
Department of Mechanical Engineering
Temple University
1947 North 12th Street, Philadelphia, PA 19122, USA
E-mail: jieyin@temple.edu
Prof. S. Yang
Department of Materials Science and Engineering
University of Pennsylvania
3231 Walnut Street, Philadelphia, PA 19104, USA
Prof. Y. K. Yi
School of Architecture
University of Illinois at Urbana–Champaign
Champaign, IL 61820, USA
Prof. R. D. Kamien
Department of Physics and Astronomy University of Pennsylvania
209 South 33rd Street, Philadelphia, PA 19104, USA

DOI: 10.1002/adma.201604262

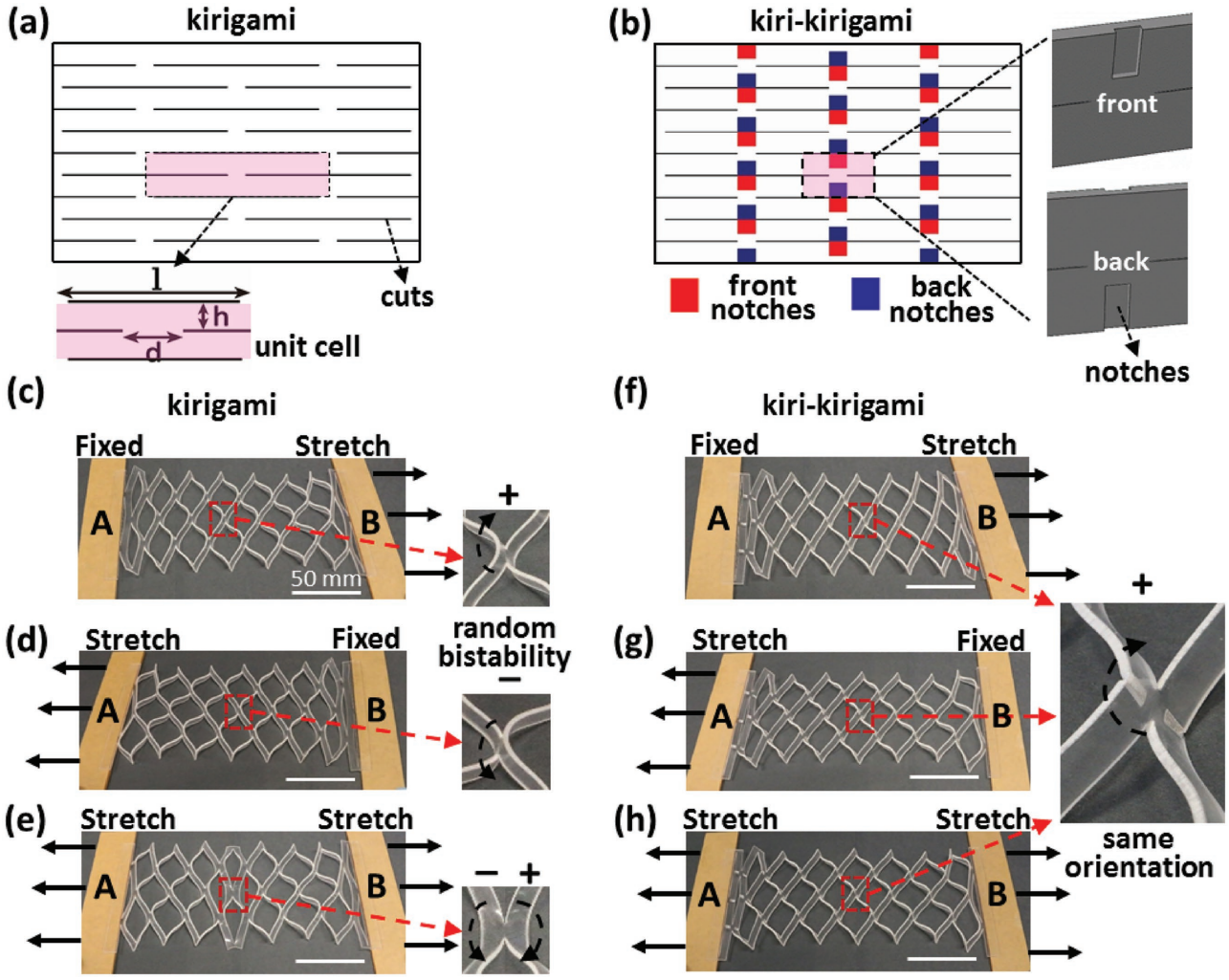

Figure 1. Indeterminate versus deterministic tilting orientations in kirigami and kiri-kirigami metamaterials, respectively. a,b) Schematic illustrations of the linearly cut kirigami structure without engraved notches (a) and with patterned notches on both sides in a kiri-kirigami structure (b). The unit cell of kirigami is highlighted in pink in (a). The red and blue rectangles in (b) represent notches on the frontside and reverse side, respectively, which are illustrated in a 3D view on the right of (b). c–e) Three expanded configurations for uniaxial stretching the same kirigami structure in (a) in different ways, showing different orientations of the unit cells represented by "+" and "−". f–h) Identical expanded configurations when uniaxially stretching the same kiri-kirigami structure in (b) in different ways, showing the same orientation of the unit cells.

(Figure 1f–h and Video S2, Supporting Information). Similar transitions from indeterminate (kirigami structure) to deterministic (kiri-kirigami structure) tilting orientations are also observed in a sheet of hardcopy paper after introducing patterned notches (Figure S1, Supporting Information). Controllable uniform tilting direction can reflect the light or solar heat either back out or inside and thus holds potential for energy saving.

To understand the observed transition from indeterminate to deterministic tilting orientations in experiments, we use FEM to simulate the buckling/tilting process (see the Experimental Section for details). For each cut unit of the kirigami structure without notches, we find bistable behavior: the unit buckles with its orientation tilting either clockwise or counterclockwise, both of which are energetically equivalent. The experimentally observed homogeneous (Figure 1c,d) and dual reverse orientations (Figure 1e) in the same kirigami structure are well captured by FEM simulation, corresponding to the first and second buckling deformation eigenmode, respectively (Figure S2, Supporting Information). Though, in principle, there is a neighbor–neighbor effect, we find that the critical buckling eigenvalue of these two modes are close to each other and lead to the indeterminate structural configurations observed in experiments. In practice, the buckling induced tilting direction of a perfect kirigami structure without geometrical imperfections is highly dependent on slight perturbations of applied forces and material inhomogeneity. In the kirigami structures we studied (Figure 1c–e), the end of the kirigami sheet was slightly lifted by the rigid attached clamp before stretching and thus provided a biased force direction creating a bending moment to induce a preferred tilting orientation (Figure S3a, Supporting Information); different tilting directions were observed depending on the direction of the applied force. However, for the kiri-kirigami structure, the

notches themselves play the role of geometrical imperfection. Notches break the deformation symmetry and generate an additional bending moment (Figure S3b, Supporting Information) to close the grooves, triggering buckling along the desired orientation that is independent of the biased direction of the applied forces. Therefore, the deformed configuration of the kiri-kirigami structure can be determined by the patterning of notches. This is confirmed by the postbuckled configuration predicted by simulation (Figure S4, Supporting Information) and is in good agreement with experiments.

The approach of using notches to direct the tilting direction makes it possible to program kiri-kirigami metamaterials with any desired patterning of clockwise or counter-clockwise local tilting orientations. "Programmability" is defined in terms of the targeted programmable tilting orientation in each element of the kiri-kirigami metamaterials through prescribed patterning of notches. Thus, potentially, a kiri-kirigami building envelope could reflect both the indoor and outdoor light on demand depending on season and local solar and lighting conditions. To generate similar configuration as in Figure 1e with dual opposite tilting orientations, the top half is designed to tilt clockwise (colored in green) through patterned double-sided notches as schematically shown in **Figure 2**a. By repeating the same patterning of the top half but with switched front and back notches, the bottom half is designed to tilt counter clockwise (colored in yellow). The design in Figure 2a is validated by uniaxially stretching the corresponding metamaterials in experiments (see Figure 2b). The opposite tilting directions lead to a high optical contrast of bright and dark pattern in the PDMS sample, where the white color at the cross-sections is generated by a laser cutter and PDMS itself is transparent (right of Figure 2b), appearing as bright and dark on the top and bottom halves, respectively. Similarly, as demonstrated in Figure 2c–e, more complicated configurations with heterogeneous tilting orientations (represented by yellow and green color) can be acquired by engineering localized patterning of notches, for example, in the form of horizontal (Figure 2c) and vertical (Figure 2d) stripes, as well as the letter T-shape (Figure 2e), displaying alternatively dark and bright stripes, and letter "T" upon uniaxial stretching due to the optical contrast of reversed tilting

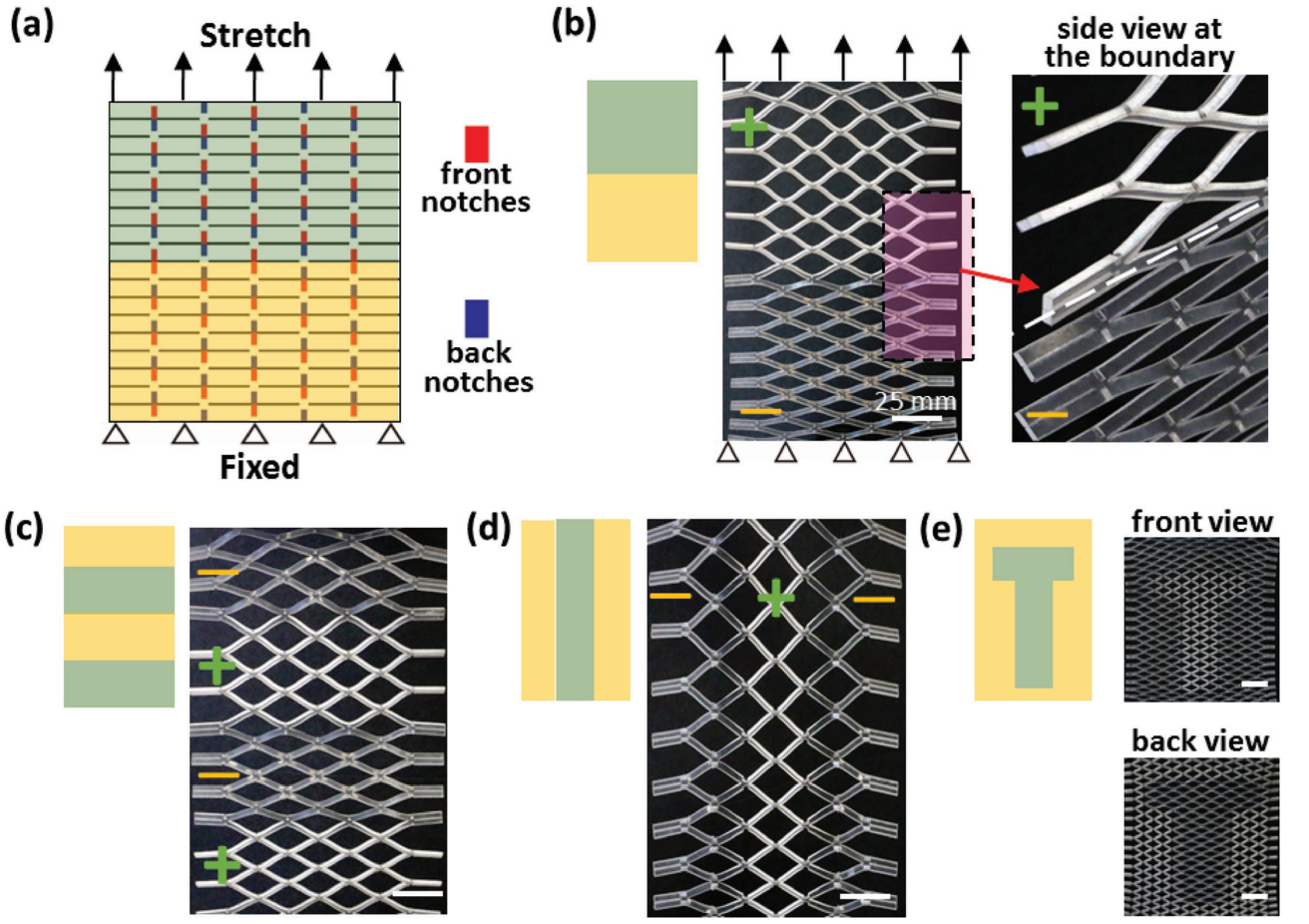

Figure 2. Programmable inhomogeneous tilting orientations in kiri-kirigami metamaterials through prescribed patterned notches. a) Schematic illustration of the kiri-kirigami with front and back notches patterned on both sides of the unit cell. The placement of notches in the top half of the sheet (highlighted in green) is reversed at the bottom half (highlighted in yellow). b) Optical images of the deformed PDMS kiri-kirigami structure upon uniaxial stretching the design in (a) showing sharp optical contrast in bright (top half) and dark (bottom). Magnified side-view optical images near the edge are shown on the right. c–e) Optical images of various configurations of stretched kiri-kirigami structures consisting of different designs of patterned notches in the form of periodic horizontal (left part of (c)) and vertical (left part of (d)) stripes, as well as letter "T" shape (left part of (e)). e) Front-view and back-view images of the letter "T" displayed in the stretched kiri-kirigami structure.

directions, respectively. Upon releasing the sample, the contrast patterns disappear (Figure S5, Supporting Information), the reversible switch of which provides potential additional functionality in optical display and even simple encryption.

Next, we examine the mechanical performance of kiri-kirigami metamaterials as potential optomechanical devices. To develop a quantitative understanding of the geometry effect of the notches on their mechanical responses, we characterized the stress–strain curves of kiri-kirigami metamaterials by varying the depth H and width W of notches (**Figure 3**a) in uniaxial tensile tests. The selected value of normalized depth H/t and normalized width W/t at 0, 0.4 (1.6), and 0.8 (4) represents no notches (kirigami structures) and notches with medium and large cut depth and width, respectively, where t is the thickness of the sheet. Compared to its counterpart, kirigami metamaterial without notches, Figure 3c,d shows the nearly identical highly nonlinear stress–strain curves over the large strain range (up to 250%) in kiri-kirigami metamaterial with medium or large notches (Figure 3c,d). Similar results are also observed in the corresponding FEM simulated stress–strain curves (the inset of Figure 3c,d), demonstrating little effect of introduced notches on its mechanical behavior within large strain ranges. The patterned cuts, however, significantly reduce the initial Young's modulus of PDMS sheet by three orders of magnitude, from ≈2 MPa (pristine without cuts and notches) to ≈2.4 kPa (after cuts).

As mentioned earlier, cuts allows for effective release of stress concentration[23,24] through out-of-plane buckling. Here we further examine the effect of notches on the stretchability, i.e., the strength of the *kirigami* metamaterials. The experimental testing is repeated over ten times for both kirigami and kiri-kirigami metamaterials. Experimental results demonstrate that the failure strain for rupture of the units is almost the same for all PDMS samples with and without notches (see examples shown in Figure S6 in the Supporting Information), somewhere between 230% and 260%. The negligible effect of notches on the failure strain is elucidated by FEM simulation. Figure 3b shows the principal stress contour of the unit for kiri-kirigami metamaterials. Similar to kirigami structures,[24] stress concentration is also observed at the cut tips in the kiri-kirigami metamaterials but without high-strain field around the engraved grooves (circled by black dash line) despite their shape changes. Therefore, as long as the grooves are positioned not too close to the cut tips, the crack will not propagate through notches, and in turn notches will not affect the strength of the kiri-kirigami structure.

Fortunately, the introduction of notches does affect the initial buckling behavior within the small strain range in Figure 3e, by largely reducing the critical buckling force that triggers the out-of-plane deformation. Figure 3e shows that increasing either normalized depth H/t or width W/t results in a decrease of the critical buckling force.

To better understand the effect of notches on the critical buckling behavior in kiri-kirigami structures, we develop a theoretical model of lateral-torsional elastic buckling of beams (Figure S7, Supporting Information) in the kirigami structure. For the kirigami structure without notches (Figure 1a), the critical buckling force F_{cr} can be derived as shown in Equation (1) (see the Supporting Information for details):

$$F_{cr} = \frac{16\pi}{(l-d)^2}\sqrt{EIGJ} = 4.62\pi\sqrt{\frac{\beta}{2(1+\nu)}}\frac{Eht^3}{(l-d)^2} \quad (1)$$

where EI and GJ are the bending stiffness and torsional stiffness, respectively. E and G are the Young's modulus and shear modulus, respectively, I and J are the moment of inertia and the torsion constant, respectively, l is the length of a unit cell, h is the distance between parallel cuts, d is transverse distance (parallel to the cuts) between cuts (Figure 1a), ν is the Poisson's ratio, and β is a constant determined by the ratio of h/t ($\beta = 1/3$ when t is small compared to h).

Although Equation (1) works for the perfect kirigami structure without notches, it can still shed some useful light on the buckling behavior of kiri-kirigami structures. Equation (1) shows that the critical buckling force is linearly proportional to the bending stiffness of the cut unit scaling with Eht^3[3] and inversely proportional to the square of the effective length of cut unit ($l - d$), indicating that thickness and cut length play a dominant role in determining the critical buckling force. When notches are introduced to the perfect kirigami structures, it will reduce the local bending stiffness of the cut unit EI by means of either deepening (i.e., increasing H in Figure 3c) or widening (increasing W in Figure 3d) the size of notches, thus, lowering the critical buckling force, which is consistent with FEM simulation (Figure 3e).

The ability to reduce the critical buckling force provides an effective way to generate open and closed kirigami structures with tilting features in thick panels,[35] which are often used in dynamic façades in buildings. It should be noted that the thickness here is not an absolute value but a relative one normalized by the parallel distance h between cuts, i.e., t/h. For a thin kirigami panel ($t/h << 1$), buckling occurs at the very beginning of the deformation due to low critical buckling force.[24] As t/h increases, it becomes more difficult to buckle out of plane. In an extreme case, a thick kirigami panel with $t/h = 1$ as shown in Figure 3f ($h = t = 1.8$, $l = 24.78$, and $d = 1.93$ mm), the PDMS kirigami structure undergoes in-plane pure bending without out-of-plane buckling (top of Figure 3f), and no out-of-plane tilting upon stretching even until rupture (at a strain of 237%). However, after introducing patterned notches ($H = 1.44$ mm, $W = 1.20$ mm), out-of-plane tilting deformation induced by rotations (bottom of Figure 3f) occurs at a relatively small strain (≈11%) due to the significantly reduced critical buckling strain enabled by notches. The strategy of imparting notches makes it possible to overcome the challenge of bending and folding thick panels[35] owing to extremely high bending stiffness.

We now consider a particular adaptive programmable kiri-kirigami metamaterial that can spontaneously tilt in a predefined direction in response to environmental temperature change, which could find potential applications in design of active environmental responsive building skins for energy saving.[30,31] By attaching thermally shrinkable tapes (highlighted in black in **Figure 4**a) to cover the patterned notches, we can remotely actuate the programmable tilting orientations of kiri-kirigami structures through temperature. Locally, it will form a self-folding bilayer structure due to the mismatched deformation between heat-induced shrinkable tapes and non-responsive constituent materials of kiri-kirigami structures.

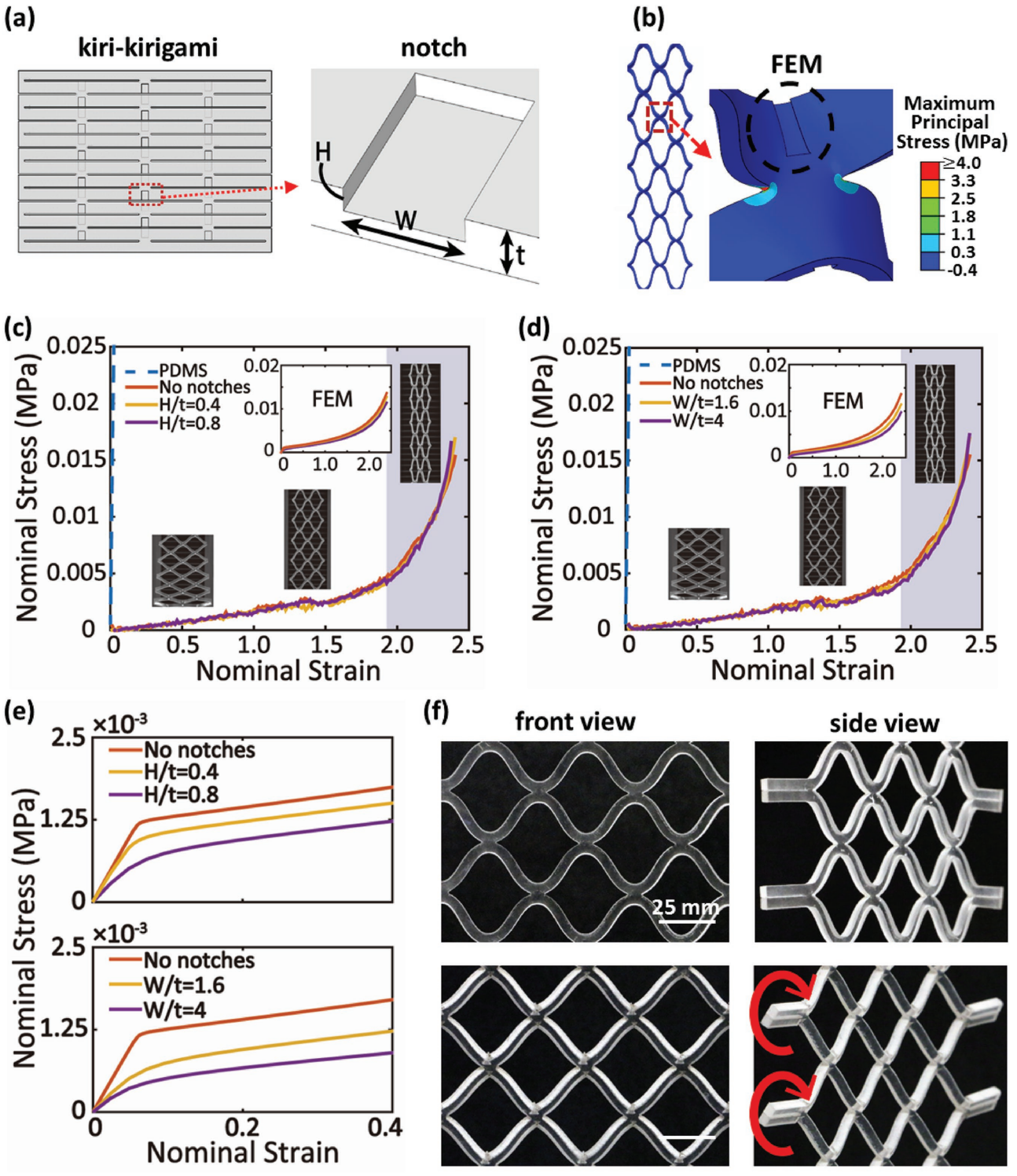

Figure 3. Effect of patterned notches on the mechanical behavior of kiri-kirigami metamaterials. a) Schematic illustration of the notch dimension with depth H and width W in a kiri-kirigami structure. b) FEM simulated stress contour of the kiri-kirigami structure, showing no stress concentration at the engraved groove highlighted by the dashed line circle. c–d) Measured nominal uniaxial stress–strain curves in kiri-kirigami metamaterials made of PDMS (l = 59.15 mm, h = 7.09 mm, d = 5.91 mm, and thickness t = 1.5 mm) as a function of the notch dimensions H (c) and W (d). Insets show the optical images of structural configurations at different level of strains. The top-right insets show the corresponding FEM simulated stress–strain curves. e) The simulated initial stress–strain curves (the applied strain ≤ 40%) of (c) and (d). f) Top: Front-view (left) and side-view (right) optical images of a PDMS-based kirigami structure with thick normalized thickness (h/t = 1) upon uniaxial stretching, showing in-plane bending only. Bottom: Front-view (left) and side-view (right) optical image of the kiri-kirigami structure as seen in (a), showing out-of-plane buckling. The red arrows represent the out-of-plane rotation directions.

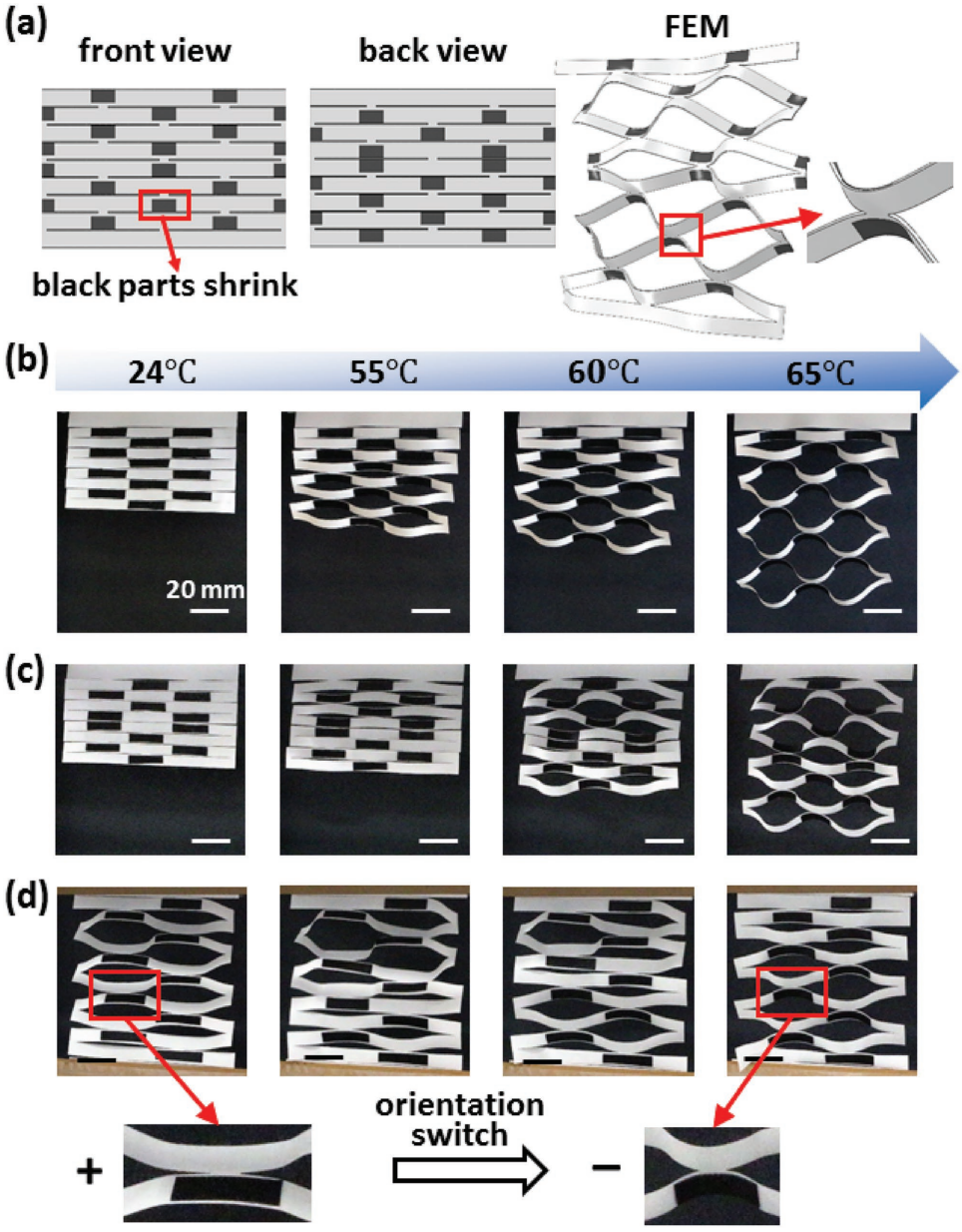

Figure 4. Remote actuation of adaptive programmable kiri-kirigami metamaterials through temperature. a) Left: Schematic illustration of design of thermally actuating kiri-kirigami structure with dual tilting orientations by covering double side notches with thermal-induced shrinkage materials (shown as black). Right: Corresponding FEM simulated expanded configuration of the designed kiri-kirigami structure in the left at an elevated temperature. b–d) Experimental demonstrations of thermal actuation of kiri-kirigami paper metamaterials with different prescribed tilting orientations when heat-shrinkable tapes (shown as black) are attached. Evolution of their structural reconfigurations as a function of temperature with monotonic (b) and dual tilting (c) orientations as well as an orientation switch (d).

Upon thermal actuation, the local self-folding leads to the spontaneous tilting of local cut units, thus collectively opening and closing the whole structure. The right of Figure 4a demonstrates the same FEM simulated kiri-kirigami structure with dual tilting orientations using remote thermal actuation as Figure 2b generated through mechanical stretching. Compared to bilayer folding without notches, the notches can help to reduce the activation strain for self-folding (Figure S8, Supporting Information), and thus potentially lowering the actuation environmental temperature.

Experimentally, polyolefin tapes (appearing black) are applied to the kiri-kirigami paper as shown in the left column of Figure 4b,c. Upon heating to 65 °C, the polyolefin tape shrinks by 5% uniaxially, leading to a nominal structural expansion strain over 80% in the kiri-kirigami paper. Using this method, we successfully demonstrate the self-expansion and programmable self-tilting of kiri-kirigami structures in response to environmental temperature with single- (Figure 4b) and dual-tilting orientations (Figure 4c and Video S3, Supporting Information).

In addition to the programmable tilting orientation through patterned local actuation, it also allows the kiri-kirigami structure to switch from one orientation (clockwise) to the other (counter-clockwise) or vice versa. At room temperature, a kiri-kirigami structure with patterned heat-shrinkable tapes was first prestretched to a strain of 10% with a specified orientation (clockwise) and then clamped on both sides (left of Figure 4d). The tapes remained straight due to their much higher stiffness compared to paper. Upon elevating the temperature, the tapes started to shrink, resulting in an abrupt switch of the bending direction from clockwise to counter-clockwise. As a result, the original orientation of deformed kiri-kirigami structure (clockwise) is switched to its opposite state (counter-clockwise) when heated and this process occurs abruptly, showing a dynamic bistability. Similar abrupt orientation switching is also observed in FEM simulation (see Figure S9 and Video S4, Supporting Information).

Armed with the knowledge of how to control the tilting feature of kiri-kirigami structures through passive and active actuation, we further explore one of the potential applications of kiri-kirigami envelopes coated with reflective coatings as a smart façade or window in reflecting and redirecting the sunlight for building energy saving.[30,31] For simplicity, here we only investigate the kiri-kirigami structure with homogenous and well-designed tilting direction. Daylight control is investigated and simulated using bidirectional transmittance distribution functions model,[36] where the value of precalculated reflectance factors of different surfaces is applied throughout the whole year. The dimension of the test case space is 5200 mm (L) × 3400 mm (W) × 2300 mm (H) as shown in **Figure 5**a composed of interior walls and three windows on the south side. The size of each window is 2300 mm (L) × 580 mm (W). Here we consider two models: one is the base model without kiri-kirigami envelopes applied to the windows (Figure 5a); the other is the proposed model with kiri-kirigami envelopes applied to the windows (Figure 5b).

As a visualization of different daylight conditions, Figure 5c,d shows the comparison of typical daylight rendering images between the two configurations using the base and proposed models, respectively. It shows the rendering images at noon of December 21 in Philadelphia, PA, USA as an example based on TMY3 (typical meteorological year) collection weather data, an average historical solar radiance in the region at this time of the year. In the base model without kiri-kirigami envelopes, Figure 5c shows that significant direct sunlight penetrates into the test space, which causes glare. In contrast, Figure 5d shows the kiri-kirigami envelope diffuses the sunlight around the window area and thus reduces the penetration of direct sunlight into the room.

The savings in electric light, cooling load, and heating load over the whole year are evaluated and compared for buildings with and without kiri-kirigami envelopes applied to windows. The simulation results are summarized in **Table 1**. The electric light saving is evaluated by the use of only natural sunlight for lighting without additional artificial lighting. The base indoor light level (illuminance) was set to be 300 lux. If indoor light level provides sufficient amount from natural daylight by adjusted kiri-kirigami structure, artificial light will be turned off. Our calculation shows that over the entire year, the use of kiri-kirigami envelopes can save electricity by about 26%

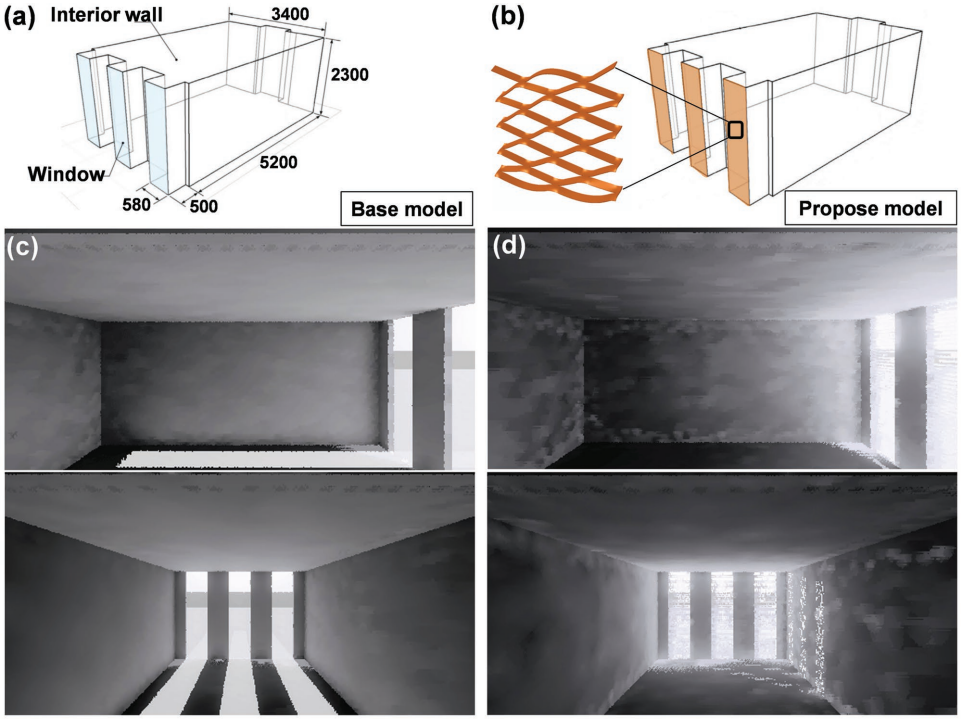

Figure 5. Building energy simulation results on the kiri-kirigami metamaterials as building skins. a,b) Illustration of a test case space without (a) (base model) and with kiri-kirigami envelopes (b) (proposed model) applied to windows. Units are mm. c,d) Rendering images of the test space in the base (c) and the proposed model (d) (a tilting angle of 30°) at noon on December 21 in Philadelphia, PA, USA.

Table 1. Comparison between base model (without kiri-kirigami envelope) and proposed model (with a kiri-kirigami envelope) in annual building energy saving. Difference = {1 − [(Proposed − Base)/Base]} × 100%.

Energy saving (unit: kWh year^{-1})[a)]	Base	Proposed (kiri-kirigami)	Difference
Electric-light saving	216	375	26.39%
Cooling-load saving	99	151	47.47%
Heating load	38	87	–28.95%

[a)]Location: Philadelphia, PA, USA.

by adjusting the kiri-kirigami structure to reduce direct sunlight during the time when an indoor illuminance is too bright (occupants usually completely block the light and use artificial light instead).

As discussed before, a kiri-kirigami envelope diffuses the daylight and reduces the heat gain. In summer, it will reduce the cooling load, thus leading to a significant saving, 47.4% more than without kiri-kirigami envelope as shown in Table 1. Here, the cooling load saving is evaluated by how much electricity can be saved through controlling the direct solar radiance passing through the windows. Blocking or diffusing solar radiance before it enters the room reduces cooling load, lowering air conditioner electricity usage. In winter, however, if one were to keep the same tilting direction, the light diffused through the kiri-kirigami envelope will increase the heating load in winter, 29% more than without the kiri-kirigami envelope. Here, the heating load is defined as the amount of energy needed to heat the space to the indoor heating setpoint temperature (e.g., 20 °C or 68 °F) using heating systems such as furnaces.

In our proof-of-concept experiments in thermal actuation of paper kiri-kirigami metamaterials, their opening and closing is irreversible unless all the tape is removed. By replacing the heat-shrink tape with reversibly responsive materials such as shape memory polymers[37] or by using other means of external stimuli such as magnetic fields, we can reversibly switch the kiri-kirigami structures. For example, by embedding magnetic inclusions in the struts between cuts, it is possible to reversibly tilt the struts out-of-plane by application of a magnetic field, similar to the remote magnetic actuation of rigid-rotation-based smart metamaterials.[38] In addition, despite the fixed tilting angle of the cut unit used in the building energy simulation (limited by the simulation tools), the kiri-kirigami envelope still shows impressive energy saving in cooling and electric lighting. We envisage that the dynamically tunable tilting angle in kiri-kirigami envelopes, controlled either through passive mechanical stretching or through active response to environmental climate changes, will further optimize the energy saving in lighting, cooling, and heating for both summer and winter. Furthermore, controllable tilting orientation to reflect either indoor or outdoor light in selected regions will largely improve personalized local comfort in the indoor environment with less energy consumption.[32]

In conclusion, by introducing patterned notches or attaching thermally responsive materials to kiri-kirigami metamaterials, we can guide the tilting direction of cut units and program/switch the expanded kiri-kirigami structures with controllable homogeneous or inhomogeneous tilting orientations. Through building energy simulation, we demonstrate the potential application of kiri-krigami structures as building envelopes to reduce energy consumption. The engraving approach can be easily extended to other 3D kirigami and origami structures, where deterministic bending or folding can be precisely controlled and programmed by engineering notches or cuts. The spontaneous tilting and expanding of programmable kiri-kirigami structures via local actuation can be applied to other responsive materials such as light-responsive materials. The dynamic tilting, opening, and close of programmable kirigami structures in response to strain or climate change open a potentially new and simple platform for designing new smart building skins for adaptive architecture for energy efficiency and sustainability. Although all the experiments only discuss programmable kiri-kirigami metamaterials at the macroscale, this technique is readily scaled down to the micro- and nanoscale for a broad range of potential applications in energy storage devices, foldable and bendable microrobots, and optoelectronic devices.

Experimental Section

Sample Fabrication: PDMS kirigami and kiri-kirigami were prepared from SYLGARD 184 silicone elastomer kit (Dow Corning) in which the precursor and the curing agent were mixed at the weight ratio of 10:1 and cured at 70 °C in oven for 2 h. Thermally responsive kiri-kirigami structures were prepared by attaching polyolefin heat-shrink tape (FIX-105-25-0) on the cut paper using glue (LOCTITE 409) and cured at 40 °C in oven for 12 h to ensure maximum bonding. All kiri-kirigami samples were fabricated using laser cut (EPILOG LASER 40 W) to generate cuts and engraved notches.

Uniaxial Tensile Test: The samples were tested using Instron 5944 with a 2 kN loading cell to characterize the stress–strain behaviors at an extension rate of 6 mm min^{-1}.

Actuation of Kiri-Kirigami Structures: The kiri-kirigami samples were hung in a transparent home-made oven and heated to 65 °C. Temperature in the oven was measured to be uniform during heating. Videos of the experiments can be found in the Supporting Information.

Finite Element Simulation: Mechanical behavior of PDMS-based (kiri-) kirigami was simulated considering the nonlinear effect of large deformations. In actuation of kiri-kirigami structures, papers, and polyolefin tapes were modeled as linear elastic materials. To capture the dynamic switching of the tilting direction in adaptive kiri-kirigami structures, the analysis was divided into two steps. In the first step, kiri-kirigami structure was stretched without being thermally actuated. In the second step, the axial boundaries were fixed and the shrinking parts were activated through temperature.

Building Energy Simulation: For energy performance in a building, we used simulation tool Sensor Placement + Optimization Tool (SPOT)[39] by using RADIANCE and DOE2. The test location was Philadelphia, PA, USA and hourly base whole year sky conditions for the simulation were generated based on the Perez All-Weather Sky Model.[40] Based on simple measurements using an illuminance meter and a reference reflector, the approximate reflectance of the walls, ceiling, and floor were determined (Table S1, Supporting Information). The transmittance of the glazing was provided through the manufacturer's specifications. Daylight simulation parameters were set high enough to increase the accuracy of the RADIANCE model. Tests were conducted on the deployed kiri-kirigami envelope wrapped around the window (Proposed) in comparison with the one without the kiri-kirigami envelope (Base). To calculate annual light savings in the model, one photo sensor was set to detect the illuminance level in the indoor space, which in turn decided to turn on/off (300 lux) the artificial light switch.

Supporting Information

Supporting Information is available from the Wiley Online Library or from the author.

Acknowledgements

J.Y. acknowledges the funding support from the start-up at Temple University. S.Y. and R.D.K. acknowledge support from National Science Foundation (NSF) Emerging Frontiers in Research and Innovation—*Origami* Design for Integration of Self-assembling Systems for Engineering Innovation (EFRI-ODISSEI) Grant No. EFRI 13-31583. This work was also partially supported by the NSF/DMR Polymer program, No. DMR-1410253 (S.Y.) and a Simons Investigator Grant from the Simons Foundation (R.D.K.).

Received: August 9, 2016
Revised: October 24, 2016
Published online: December 27, 2016

[1] D. Chwieduk, *Appl. Energy* **2003**, *76*, 211.
[2] H. F. Castleton, V. Stovin, S. B. M. Beck, J. B. Davison, *Energy Build.* **2010**, *42*, 1582.
[3] S. B. Sadineni, S. Madala, R. F. Boehm, *Renewable Sustainable Energy Rev.* **2011**, *15*, 3617.
[4] A. Azens, C. Granqvist, *J. Solid State Electrochem.* **2003**, *7*, 64.
[5] D. Ge, E. Lee, L. Yang, Y. Cho, M. Li, D. S. Gianola, S. Yang, *Adv. Mater.* **2015**, *27*, 2489.
[6] A. V. Thomas, B. C. Andow, S. Suresh, O. Eksik, J. Yin, A. H. Dyson, N. Koratkar, *Adv. Mater.* **2015**, *27*, 3256.
[7] J. Y. Ou, E. Plum, L. Jiang, N. I. Zheludev, *Nano Lett.* **2011**, *11*, 2142.
[8] A. Q. Liu, W. M. Zhu, D. P. Tsai, N. I. Zheludev, *J. Optics* **2012**, *14*, 114009.
[9] J. P. Turpin, J. A. Bossard, K. L. Morgan, D. H. Werner, P. L. Werner, *Int. J. Antennas Propag.* **2014**, *2014*, 18.
[10] N. I. Zheludev, E. Plum, *Nat. Nanotechnol.* **2016**, *11*, 16.
[11] J.-H. Lee, J. P. Singer, E. L. Thomas, *Adv. Mater.* **2012**, *24*, 4782.
[12] D. Attard, J. N. Grima, *Phys. Status Solidi B* **2008**, *245*, 2395.
[13] M. R. Dudek, K. W. Wojciechowski, J. N. Grima, R. Caruana-Gauci, K. K. Dudek, *Smart Mater. Struct.* **2015**, *24*, 085027.
[14] S. Babaee, J. Shim, J. C. Weaver, E. R. Chen, N. Patel, K. Bertoldi, *Adv. Mater.* **2013**, *25*, 5044.
[15] B. Florijn, C. Coulais, M. van Hecke, *Phys. Rev. Lett.* **2014**, *113*, 175503.
[16] J. L. Silverberg, A. A. Evans, L. McLeod, R. C. Hayward, T. Hull, C. D. Santangelo, I. Cohen, *Science* **2014**, *345*, 647.
[17] C. Lv, D. Krishnaraju, G. Konjevod, H. Yu, H. Jiang, *Sci. Rep.* **2014**, *4*, 5979.
[18] E. T. Filipov, T. Tachi, G. H. Paulino, *Proc. Natl. Acad. Sci. USA* **2015**, *112*, 12321.
[19] M. Eidini, G. H. Paulino, *Sci. Adv.* **2015**, *1*, e1500224.
[20] J. T. B. Overvelde, T. A. de Jong, Y. Shevchenko, S. A. Becerra, G. M. Whitesides, J. C. Weaver, C. Hoberman, K. Bertoldi, *Nat. Commun.* **2016**, *7*, 10929.
[21] Y. Cho, J.-H. Shin, A. Costa, T. A. Kim, V. Kunin, J. Li, S. Y. Lee, S. Yang, H. N. Han, I.-S. Choi, D. J. Srolovitz, *Proc. Natl. Acad. Sci. USA* **2014**, *111*, 17390.
[22] Y. Tang, G. Lin, L. Han, S. Qiu, S. Yang, J. Yin, *Adv. Mater.* **2015**, *27*, 7181.
[23] M. K. Blees, A. W. Barnard, P. A. Rose, S. P. Roberts, K. L. McGill, P. Y. Huang, A. R. Ruyack, J. W. Kevek, B. Kobrin, D. A. Muller, P. L. McEuen, *Nature* **2015**, *524*, 204.
[24] T. C. Shyu, P. F. Damasceno, P. M. Dodd, A. Lamoureux, L. Xu, M. Shlian, M. Shtein, S. C. Glotzer, N. A. Kotov, *Nat. Mater.* **2015**, *14*, 785.
[25] Z. Song, X. Wang, C. Lv, Y. An, M. Liang, T. Ma, D. He, Y.-J. Zheng, S.-Q. Huang, H. Yu, H. Jiang, *Sci. Rep.* **2015**, *5*, 10988.
[26] T. Castle, Y. Cho, X. Gong, E. Jung, D. M. Sussman, S. Yang, R. D. Kamien, *Phys. Rev. Lett.* **2014**, *113*, 245502.
[27] D. M. Sussman, Y. Cho, T. Castle, X. Gong, E. Jung, S. Yang, R. D. Kamien, *Proc. Natl. Acad. Sci. USA* **2015**, *112*, 7449.
[28] Y. Zhang, Z. Yan, K. Nan, D. Xiao, Y. Liu, H. Luan, H. Fu, X. Wang, Q. Yang, J. Wang, W. Ren, H. Si, F. Liu, L. Yang, H. Li, J. Wang, X. Guo, H. Luo, L. Wang, Y. Huang, J. A. Rogers, *Proc. Natl. Acad. Sci. USA* **2015**, *112*, 11757.
[29] A. Lamoureux, K. Lee, M. Shlian, S. R. Forrest, M. Shtein, *Nat. Commun.* **2015**, *6*, 8092.
[30] A. E. D. Grosso, P. Basso, *Smart Mater. Struct.* **2010**, *19*, 124011.
[31] R. C. G. M. Loonen, M. Trčka, D. Cóstola, J. L. M. Hensen, *Renewable Sustainable Energy Rev.* **2013**, *25*, 483.
[32] J. Lovell, *Building Envelopes: An Integrated Approach*, Princeton Architectural Press, New York **2010**.
[33] Y. Han, Y. Shokef, A. M. Alsayed, P. Yunker, T. C. Lubensky, A. G. Yodh, *Nature* **2008**, *456*, 898.
[34] S. H. Kang, S. Shan, A. Košmrlj, W. L. Noorduin, S. Shian, J. C. Weaver, D. R. Clarke, K. Bertoldi, *Phys. Rev. Lett.* **2014**, *112*, 098701.
[35] Y. Chen, R. Peng, Z. You, *Science* **2015**, *349*, 396.
[36] P. K. Acharya, A. Berk, G. P. Anderson, G. P. Anderson, N. F. Larsen, S. C. Tsay, K. H. Stamnes, *Proc. SPIE* **1999**, *3756*, DOI:10.1117/12.366389.
[37] M. Behl, K. Kratz, J. Zotzmann, U. Nöchel, A. Lendlein, *Adv. Mater.* **2013**, *25*, 4466.
[38] N. G. Joseph, C.-G. Roberto, R. D. Mirosław, W. W. Krzysztof, G. Ruben, *Smart Mater. Struct.* **2013**, *22*, 084016.
[39] Daylight Innovations website, https://www.daylightinnovations.com/spot-home, acessed: June **2016**.
[40] R. Perez, R. Seals, J. Michalsky, *Sol. Energy* **1993**, *50*, 235.